

# Preparation and Characterization of Poly(3-arylthiophene)s

Douglas J. Guerrero, Xiaoming Ren, and J. P. Ferraris\*

Department of Chemistry, The University of Texas at Dallas, P.O. Box 830688,  
Richardson, Texas 75083-0688

Received February 3, 1994. Revised Manuscript Received April 22, 1994\*

A series of 3-(*p*-X-phenyl)thiophene monomers (X = -CMe<sub>3</sub>, -Me, -OMe, -H, -F, -Cl, -Br, -CF<sub>3</sub>, -SO<sub>2</sub>Me) was electrochemically polymerized to form polymer films that could be reversibly reduced and oxidized (n- and p-doped). The oxidation potentials of the monomers and formal potentials of the n- and p-doping processes of polymers were correlated with the resonance and inductive effects of the substituents on the phenyl ring. The charge obtained by integrating the cyclic voltammetric peak was affected by the polymerization efficiency and, in some cases, the ion transport rate. The ionic resistance of poly[3-(*p*-chlorophenyl)thiophene] (PCPT) and poly[3-(*p*-fluorophenyl)thiophene] (PFPT) films measured by impedance spectroscopy, together with scanning electron microscopy results, demonstrate that the ion transport in these films is affected by their morphology.

## Introduction

Conducting polymers have attracted much recent attention due to their potential use in rechargeable batteries,<sup>1</sup> electrochromic display devices,<sup>2</sup> and supercapacitors.<sup>3</sup> Polyheterocycles have become important in these areas due to their facile electrochemical polymerization and doping, with polythiophenes exhibiting especially promising properties in their conducting and neutral states.<sup>4</sup> Although p-type doping has been well researched, n-type doping studies are comparatively rare due to the poor stability of the polymers at the extreme negative potentials. Nevertheless materials that exhibit both p- and n-doping capabilities will be important for constructing type III capacitors,<sup>5</sup> in which one electrode is p-doped and the other is n-doped when the capacitor is charged. As we reported earlier,<sup>5</sup> this type of capacitor has the potential advantages of high energy density ( $E = 1/2CV^2$ ) due to the high cell voltage ( $\approx 3$  V) and high power density resulting from the fast release of stored charge since both electrodes are doped and highly conductive. Although we had previously identified poly[3-(*p*-fluorophenyl)thiophene] as a promising candidate for such devices,<sup>5</sup> we recognized that optimization of the polymeric materials' performance would require the elucidation of those factors that influence charge storage and release, cyclability and long-term stability and hence began this study.

Sato et al.<sup>6</sup> have found that poly(3-phenylthiophene) (PPT) is highly p-dopable and also suggested its application in a p-n junction diode (although the reported doping levels might be highly overestimated<sup>7</sup>). The high

p-doping activity of PPT was explained in terms of a favorable conjugation effect between the phenyl rings and the polythiophene backbone.<sup>8</sup> Recently, Onoda et al.<sup>9</sup> studied the n-doping properties of PPT films and found a high degree of electrochemical reversibility. However, this group concluded that rather than being in conjugation with the polythiophene backbone, the phenyl rings were perpendicular to it<sup>9</sup> and the observed electronic properties were limited by the interchain charge-transport processes. Sato et al.<sup>8</sup> further demonstrated the oxidation potential of PPT increased when an electron-withdrawing substituent was placed on the phenyl ring (e.g., poly[*p*-trifluoromethylphenyl]-3-thiophene], PTFMT) and electron-donating groups (e.g., poly[*p*-methoxyphenyl]-3-thiophene], PMPT) produced a stable anion-doped material.<sup>10</sup>

To determine the role that the (substituted) phenyl groups play during the n- and p-doping processes, we examined a series of para-substituted-3-phenylthiophenes where the substituent was -CMe<sub>3</sub>, -Me, -OMe, -H, -F, -Cl, -Br, -CF<sub>3</sub>, or -SO<sub>2</sub>Me. We report here the results of cyclic voltammetry in which the redox properties of the monomers and resultant polymers were correlated with Hammett substituent constants. We also examined the factors which affect the amount of the cyclic voltammetric charge obtained for the p- and n-doping processes of the polymers. Finally, we characterized several of the polymers by impedance spectroscopy (IS) and scanning electron microscopy (SEM).

## Experimental Section

**General Data.** NMR and IR spectra were recorded on a JEOL JNM-FX270 and a Mattson Instruments 2025 Galaxy FTIR spectrometer, respectively. Elemental analyses were performed by Oneida Research Services, Inc., Whitesboro, NY. Polymer morphologies were observed on gold-sputtered samples using a Phillips XL-30 scanning electron microscope operated at an

\* Abstract published in *Advance ACS Abstracts*, August 15, 1994.

(1) Santhanam, K. S. V.; Gupta, N. *TRIP* 1993, 1 (9), 284.

(2) Panero, S.; Passerini, S.; Scrosati, B. *Mol. Cryst. Liq. Cryst.* 1993, 229, 97.

(3) (a) Huang, S. C.; Huang, S. M.; Ng, H.; Kaner, R. B. *Synth. Met.* 1993, 55-57, 4047. (b) Baughman, R. H. *Makromol. Chem., Macromol. Symp.*, 1991, 51, 193. (c) Conway, B. E. *J. Electrochem. Soc.* 1991, 138, 1539.

(4) Mastragostino, M.; Arbizzani, C.; Bongini, A.; Barbarella, G.; Zambianchi, M. *Electrochim. Acta* 1993, 38, 135.

(5) Rudge, A.; Davey, J.; Raistrick, I.; Gottesfeld, S.; Ferraris, J. P. *J. Power Sources* 1994, 47, 89.

(6) Sato, M.; Tanaka, S.; Kaeriyama, K. *J. Chem. Soc., Chem. Commun.* 1987, 1725.

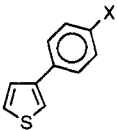
(7) Roncali, J. *Chem. Rev.* 1992, 92, 711.

(8) Sato, M.; Tanaka, S.; Kaeriyama, K. *Makromol. Chem.* 1989, 190, 1233.

(9) Onoda, M.; Nakayama, H.; Morita, S.; Yoshino, K. *Synth. Met.* 1993, 55-57, 275.

(10) Kaeriyama, K.; Tanaka, S.; Sato, M.; Hamada, K. *Synth. Met.* 1989, 28, C611.

Table 1.  $\sigma_i$ ,  $\sigma_r$ ,  $\sigma_p$ , and Oxidation Potential for Monomers and Formal Potentials of p- and n-Doping and Cycling Charges for Polymers<sup>a</sup>

monomer		Hammett values <sup>16</sup>			$E_{\text{oxidation}}$	polymer		CV charge of polymer <sup>b</sup> ( $\mu\text{C}$ )	
acronym for polymer		$\sigma_i$	$\sigma_r$	$\sigma_p$		$E_{\text{n-doping}}$	$E_{\text{p-doping}}$	n-doping	p-doping
									
-CMe <sub>3</sub>	PBPT	-0.07	-0.17	-0.24	0.943	-2.047	0.676	81.14	58.75
-Me	PMPT	-0.05	-0.13	-0.18	0.928	-2.044	0.640	18.34	11.40
-OMe	PMtPT	0.27	-0.42	-0.15	0.804	-2.088	0.626	7.327	5.737
-H	PPT	0	0	0	0.991	-1.954	0.706	29.99	39.32
-F	PFPT	0.50	-0.31	0.19	1.024	-1.968	0.697	61.33	65.17
-Cl	PCPT	0.46	-0.18	0.28	1.042	-1.919	0.770	18.94	94.61
-Br	PBrPT	0.44	-0.16	0.28	1.076	-2.033	0.694	90.05	92.34
-CF <sub>3</sub>	PTFMPT	0.42	0.08	0.50	1.016	-1.937	0.792	49.40	44.46
-SO <sub>2</sub> Me	PMSPT	0.60	0.12	0.72	1.117	-1.894	0.740	140.4	132.2
3-methylthiophene	P3MT	N/A	N/A	N/A	1.060	-2.23	0.389		
thiophene	PT	N/A	N/A	N/A	1.316	-2.05	0.622		

<sup>a</sup> N/A = not applicable. <sup>b</sup> Integrated charge of the anodic current for the p-doping (0 to 0.95 V) and the cathodic current for the n-doping (-1 to -2.1 V) processes, from the cyclic voltammograms recorded at 60 mV/s.

accelerating voltage of 15 kV. Impedance measurements were carried out using a PARC model 273A potentiostat coupled to an Schlumberger Instruments 1260 impedance/gain-phase analyzer. The experiments were controlled, and the data were collected using Zplot for Microsoft Windows (version 1.1, Scribner Associates, Inc.) installed on a IBM compatible computer. The cyclic voltammetry was performed on the same equipment without the frequency analyzer, and the data were collected and analyzed with Model 270/250 Research Electrochemistry Software (version 4.0, EG&G Instruments Inc.). All electrochemical experiments were carried out in a He-filled glovebox. A three-compartment cell consisting of a Pt working electrode (area 0.0045 cm<sup>2</sup>), a glassy carbon counter electrode, and a nonaqueous Ag/Ag<sup>+</sup> reference electrode was used. The formal potential of the ferrocene/ferrocenium couple was measured to be 0.075 V vs the reference electrode, and all the potentials reported here are quoted against the reference electrode.

Tetraethylammonium tetrafluoroborate (TEATFB, Aldrich Chemical Co.) was recrystallized three times from methanol and dried under vacuum at 120 °C for 24 h before use. A small amount of activated alumina (800 °C for 2 h) was placed in the bottom of the cell to remove residual amounts of water from acetonitrile (Aldrich Sure-Seal, 50 ppm H<sub>2</sub>O).

**Synthesis of Monomers.** 3-Substituted-thiophene monomers (1-7) were prepared by a nickel(II)-catalyzed coupling reaction as described in the literature<sup>11</sup> with yields ranging from 65 to >98%. The monomers synthesized using a multistep<sup>12</sup> method were 3-(p-bromophenyl)thiophene and 3-(p-methylthiophenyl)thiophene. The latter was used as a precursor for the synthesis of novel compound 3-(p-methylsulfonylphenyl)thiophene.

**3-(Phenyl)thiophene (1).** Purified by recrystallization from ethanol/water using decolorizing carbon followed by sublimation, mp 89.5-90.8 °C (lit.<sup>12</sup> 90-91 °C).

**3-(p-Methoxyphenyl)thiophene (2).** Purified by sublimation, mp 124-126 °C (lit.<sup>13</sup> 127 °C).

**3-(p-(Trifluoromethyl)phenyl)thiophene (3).** Purified by recrystallization from ethanol/water using decolorizing carbon followed by sublimation, mp 112.0-112.5 °C (lit.<sup>8</sup> 120.1-121.7 °C). Elemental analysis (%): calcd C 57.90, H 3.09; found, C 57.95, H 2.83. This compound gave satisfactory spectroscopic data and elemental analysis, and we suggest that there might be an error in the reported melting point.

**3-(p-tert-Butylphenyl)thiophene (4).** To our knowledge this is a novel compound, and its synthesis will be given in detail.

Diethyl ether (40 mL), 1,3-bis(diphenylphosphinopropane)-nickel(II) (0.108 g) and 3-bromothiophene (7.81 mL, 83 mmol) were placed in oven-dried glassware under N<sub>2</sub> atmosphere and cooled in an ice bath. To this mixture was added 4-(tert-butylphenyl)magnesium bromide (Aldrich Chemical Co., 50 mL, 2.0 M in Et<sub>2</sub>O, 0.100 mol). The reaction was slightly exothermic, and a dark-brown/black color developed within minutes. The mixture was refluxed for 24 h, cooled in an ice bath, and quenched with cold HCl (50 mL, 1.0 N). The water layer was separated and extracted with diethyl ether (3 × 10 mL). The combined organics were dried (MgSO<sub>4</sub>), and the solvent was removed to yield the crude product. The crude product was purified by recrystallization from ethanol/water using decolorizing carbon followed by sublimation, and a second recrystallization from ethanol affording 17.9 g (71%) of a white powder, mp 77.0-78.5 °C. <sup>1</sup>H NMR (270 MHz, CDCl<sub>3</sub>) δ 1.35 (s, 9H, CMe<sub>3</sub>), 7.38-7.55 (m, 7H, aromatic). FTIR (KBr, cm<sup>-1</sup>) 781 (vs), 1370 (m), 1419 and 1496 (m), 2960 (vs), 3092 (w). Elemental analysis (%): calcd C 77.7, H 7.45; found C 77.6, H 7.31.

**3-(p-Methylphenyl)thiophene (5).** Purified by sublimation, mp 111-113 °C (lit.<sup>14</sup> 112 °C).

**3-(p-Fluorophenyl)thiophene (6).** Purified by sublimation, mp 85.0-86.6 °C (lit.<sup>12</sup> 86-87 °C).

**3-(p-Chlorophenyl)thiophene (7).** Purified by recrystallization from ethanol/water using decolorizing carbon followed by sublimation, mp 102.0-103.0 °C (lit.<sup>12</sup> 104-105 °C).

**3-(p-Bromophenyl)thiophene (8).** Purified by sublimation, mp 122-124 °C (lit.<sup>15</sup> 124-125 °C).

**3-(p-Methylsulfonylphenyl)thiophene (9).** p-(Methylthio)phenylsuccinic acid was prepared from p-(methylthio)benzaldehyde (Aldrich) following the literature procedure described for the p-bromophenyl derivative.<sup>16</sup> p-(Methylthio)phenylsuccinic acid (2.54 g, 10.5 mmol) was converted to its sodium salt with aqueous NaOH (25 mL, 1 N) followed by the removal of water under reduced pressure. The resulting white powder was mixed with o-dichlorobenzene (25 mL), red phosphorus powder (1.2 g, 38.7 mmol), phosphorus pentasulfide (3.3 g, 14.8 mmol) and benzyltriethylammonium chloride (0.130 g, 0.57 mmol). This mixture was heated to 130-140 °C overnight and filtered while hot. The remaining phosphorus salts were rinsed with CH<sub>2</sub>Cl<sub>2</sub> (2 × 10 mL). The filtrate and CH<sub>2</sub>Cl<sub>2</sub> rinse were combined and adsorbed onto neutral alumina, and the solvent was removed under reduced pressure. The resulting alumina/product powder was loaded onto a neutral alumina column and eluted with 50:50 CH<sub>2</sub>Cl<sub>2</sub>/hexanes (≈300 mL). After removal of solvent, the crude yellow powder was sublimed to yield 1.33 g (61.6%) of 3-(p-(methylthio)phenyl)thiophene as a white powder, mp 129-131

(11) Tamao, K.; Kodama, S.; Nakajima, I.; Kumada, M. *Tetrahedron* 1982, 38, 3347.

(12) Reddy Sastry, C. V.; Marwah, A. K.; Marwah, P.; Shankar Rao, G.; Shridhar, D. R. *Synthesis* 1987, 1024.

(13) Montheard, J. P.; Delzant, J. F. *Synth. Commun.* 1984, 14 (3), 289.

(14) Chrzaszczewska, A. *Rocz. Chem.* 1925, 5, 33; *Chem. Abstr.* 1926, 20, 1078.

(15) Martelli, G.; Spagnolo, P.; Tiecco, M. *J. Chem. Soc. (B)* 1968, 901.

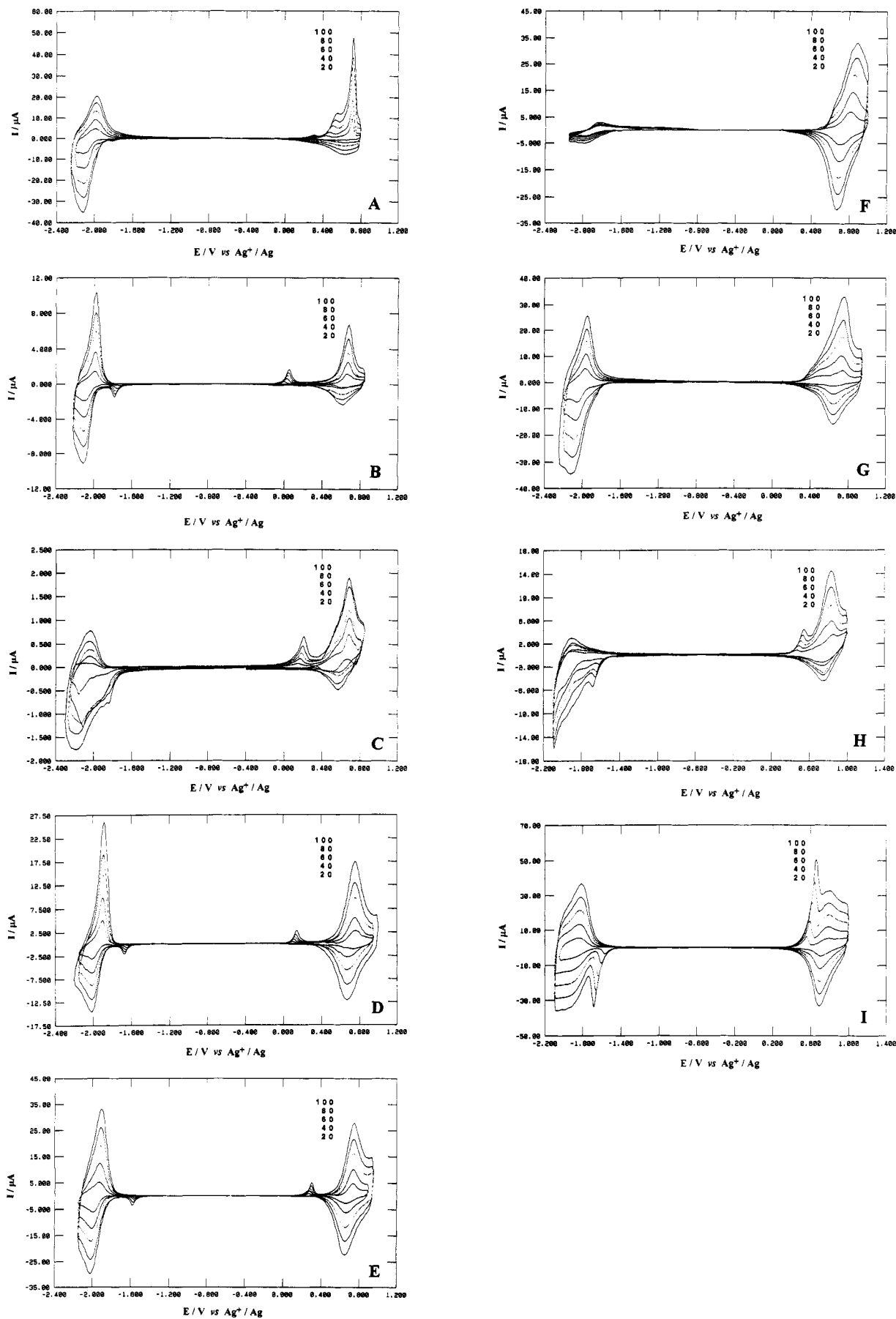


**Figure 1.** Cyclic voltammograms of polymer films coated on Pt electrodes immersed in 0.2 M Et<sub>4</sub>NBF<sub>4</sub> acetonitrile solution: (A) PBPT, (B) PMPT, (C) PMtPT, (D) PPT, (E) PFPT, (F) PCPT, (G) PBtPT, (H) PTFMPT, and (I) PMSPT, at scan rates of 20, 40, 60, 80, and 100 mV/s. See Table 1 for the acronyms of polymers.

°C.  $^1\text{H}$  NMR (270 MHz,  $\text{CDCl}_3$ )  $\delta$  2.51 (s, 3H, *SMe*), 7.26–7.54 (m, 7H, aromatic).  $^{13}\text{C}$  NMR (270 MHz,  $\text{CDCl}_3$ )  $\delta$  16.0 (1C, *SMe*), 120 (3C, ipso), 126.2–127.1 (5C, methine). FTIR (KBr,  $\text{cm}^{-1}$ ) 777 (vs), 1417 (m), 1489 (m), 2920 (w), 3094 (w). Elemental analysis (%): calcd C 64.0, H 4.9; found C 64.1, H 4.96.

3-(*p*-(Methylthio)phenyl)thiophene (0.759 g, 3.7 mmol) in acetone (10 mL) was treated with an aqueous solution of  $\text{KHSO}_5$  (oxone, 1.17 g, 7.7 mmol in 5 mL of water) and stirred at room temperature for 48 h. The reaction was quenched with water (20 mL), and the mixture was extracted with  $\text{CH}_2\text{Cl}_2$  ( $3 \times 10$  mL). The organics were dried with  $\text{MgSO}_4$ , and solvent was removed under reduced pressure to yield 0.74 g (3.1 mmol, 84%) of a crude light yellow solid of compound **9** which was further purified by recrystallization from  $\text{CH}_2\text{Cl}_2$ /methanol followed by sublimation to obtain a white powder in 69% yield (0.61 g) with mp 155.5–157.0 °C.  $^1\text{H}$  NMR (270 MHz,  $\text{CDCl}_3$ )  $\delta$  3.08 (s, 3H, *SMe*), 7.44–7.61 (m, 3H, thiophene aromatic), 7.76–7.98 (dd, 4H, phenyl aromatic). FTIR (KBr,  $\text{cm}^{-1}$ ) 771 (vs), 1145 and 1303 (vs,  $-\text{SO}_2-$ ), 1417 and 1595 (m), 2928 (w), 3011 and 3089 (w). Elemental analysis (%): Calcd C 55.4, H 4.2, S 26.9; found C 55.8, H 4.17, S 26.9.

## Results and Discussion

**Electrochemical Polymerization and Cyclic Voltammetry.** The polymers were prepared under identical conditions by anodic oxidation of their monomer solutions at a constant current density of 3.56  $\text{mA}/\text{cm}^2$  for the same deposition charge of 240  $\text{mC}/\text{cm}^2$ . Acetonitrile solutions containing 0.1 M monomer and 1.0 M  $\text{Et}_4\text{NBF}_4$  were used for the polymerization, and the cyclic voltammetry and impedance measurements were carried out in 0.2 M  $\text{Et}_4\text{NBF}_4$  acetonitrile solution. The oxidation potentials of the monomers were estimated from the electrode potential at long times ( $>300$  s) during the polymerization at a small current density of 0.44  $\text{mA}/\text{cm}^2$ . The oxidation potentials thus obtained were insensitive to the nature of the underlying substrate electrode and are close to the minimum electrode potentials required to form the polymers. It should be noted that the electrode potentials were very sensitive to the monomer concentration and the current density.

The relative efficiency of polymerization could be estimated by integrating the anodic charge from the polymer's cyclic voltammograms for the p-doping process, assuming that all polymers have the same doping level. This p-doping region was chosen since the polymer in this region has lower ionic resistance than in the n-doping region. Thus the integrated charge is less likely to be limited by slow ion transport. For films of PMtPT, PMPT, and PPT (see Table 1 for acronyms), a comparatively low p-doping charge was found. During the polymerization of these systems, soluble oligomers were observed to stray away from the electrode with subsequent coloration of the monomer solution, and the resulting polymer films were very thin. Cyclic voltammograms recorded at scan rates from 20 to 100  $\text{mV}/\text{s}$  at 20  $\text{mV}/\text{s}$  intervals are shown in Figure 1 for the polymer films studied here. Formal potentials for both p- and n-doping processes were estimated by averaging the anodic and cathodic peak potentials of each process at a scan rate of 60  $\text{mV}/\text{s}$ . Formal potentials evaluated at other scan rates were not significantly different ( $<6$  mV for most cases).

**Effect of Substitution on Redox Potentials of Monomers and Polymers.** The effects of substitution on the redox properties of the monomers and polymers stem from an interplay of steric and electronic (resonance/inductive) factors. The latter can often be estimated from

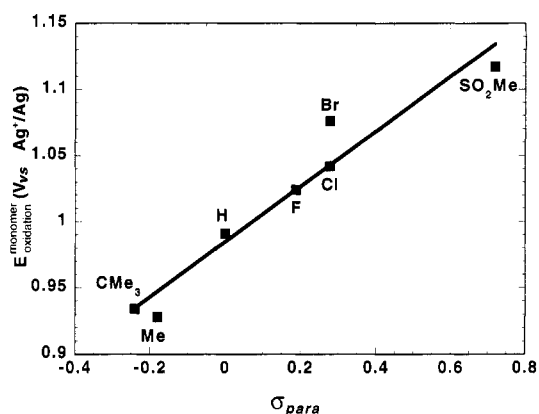


**Figure 2.** Plot of the oxidation potentials for the monomers against  $\sigma_p$  values.

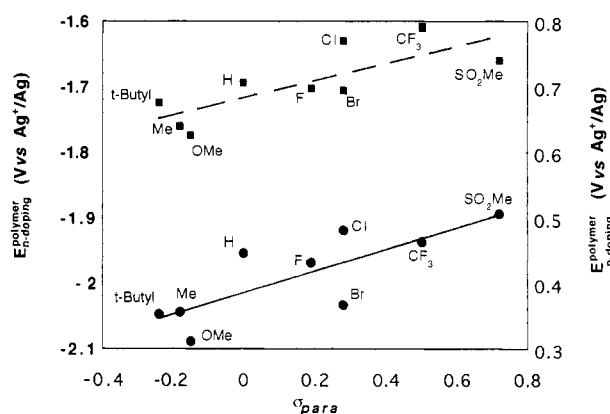


**Figure 3.** Plot of reduction and oxidation potentials for the polymers against  $\sigma_p$  values. Full squares (■) and circles (●) represent oxidation and reduction, respectively.

Hammett  $\sigma$  constants.<sup>16</sup> For the 3-arylthiophenes studied here, the substituent is in the para position, making  $\sigma_p$  [which is the sum of inductive ( $\sigma_i$ ) and resonance ( $\sigma_r$ ) contributions] the most appropriate. It is important to note that these effects do not always work in the same direction. For example, even though F is more electron withdrawing than H by induction, it donates electrons by resonance. In such cases it is difficult to predict which factor predominates. Table 1 lists the  $\sigma_i$ ,  $\sigma_r$ , and  $\sigma_p$  constants, the oxidation potentials of the monomers, and the formal oxidation and reduction potentials for their respective polymers. Preliminary results on a subset of this series have been reported.<sup>17</sup> Figures 2 and 3 show the trends in the redox properties for the monomers and polymers are as expected with the potentials shifting cathodically for electron-donating substituents ( $\sigma_p < 0$ ) and anodically for electron-withdrawing groups ( $\sigma_p > 0$ ). Both inductive and resonance effects influenced the oxidation potential of monomers. For example,  $-\text{CF}_3$  which has similar steric requirements and resonance values ( $\sigma_r$ ) as  $-\text{CH}_3$  shifts the oxidation peak to higher potential due to its higher electron-withdrawing ability. When the substituents have similar inductive values (e.g.,  $-\text{F}$  and  $-\text{Cl}$ ) the one with higher electron-donating ability (in this case  $-\text{F}$ ) shifts the oxidation potential to a lower value. The effect is more pronounced for the monomers than for

(16) March, J. *Advanced Organic Chemistry*, 4th ed.; John Wiley & Sons: New York, 1992; pp 280ff.

(17) Rudge, A., Raistrick, I., Gottesfeld, S.; Ferraris, J. P. *Electrochim. Acta* 1994, 39, 273.

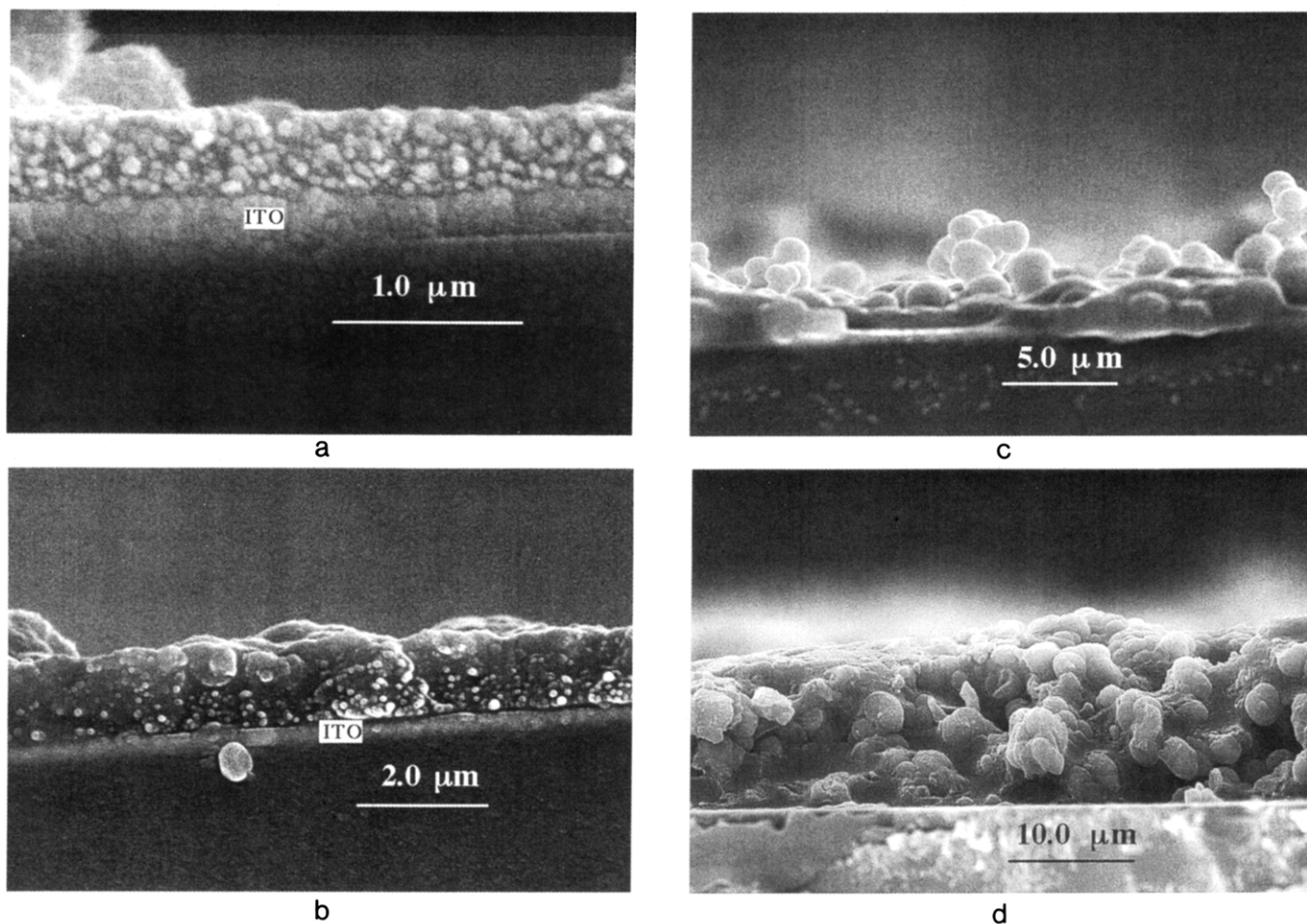


**Figure 4.** Cross sectional scanning electron micrographs of (a) PPT, (b) PFPT, (c) PCPT, and (d) PBrPT films deposited on indium tin oxide electrodes.

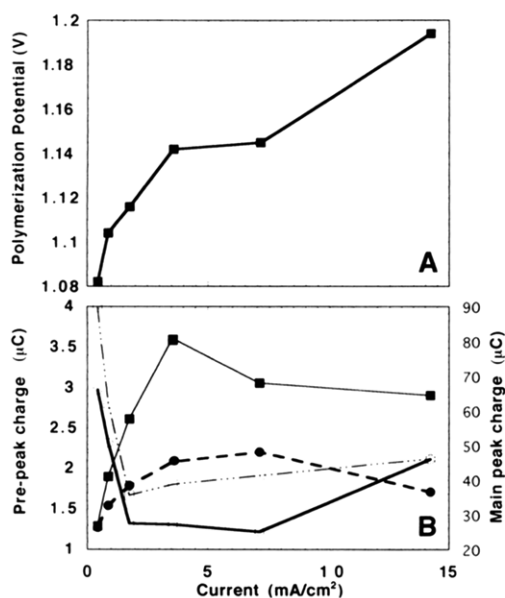


**Figure 5.** Plots of (A) polymerization potential as a function of deposition current density and (B) cyclic voltammetric charges for the prepeaks (open symbols) and main peaks (filled symbols) of the p-doping (□) and n-doping (○) of PFPT films.

the polymers (the shifts are in the order of 200–300 mV in the monomers and 50–100 mV in the polymers relative to thiophene and polythiophene, respectively), and the size of the substituent does not have a significant effect. The overall diminished substituent effect in the polymers suggests a decreased conjugation between the substituted

phenyl rings and the polythiophene backbone. Figure 3 also shows that the *difference* between the p- and n-doping formal potentials on the polymers is essentially unchanged upon substitution. This is not unexpected since the symmetries of the frontier orbitals of 3-arylthiophenes are such that the substituents can interact with both levels, shifting them downward (or upward) to comparable extents, thus the  $E_{\text{gap}}$  remains essentially the same.

#### Electrochemistry and Microscopy of Polymers.

Despite variation across the series, the cycling charges for the p-doping and n-doping processes for individual members are comparable. The one exception is PCPT which shows a very low n-doping charge compared to its p-doping charge. SEM examination of a film of this polymer deposited on an indium tin oxide (ITO) coated glass electrode showed a very dense morphology (Figure 4C) with a film thickness from one to two micrometers. This film resisted efforts to produce a clear cross section when the substrate electrode was broken at a right angle along the polymer coated surface. A PFPT film (Figure 4B) of similar thickness appeared particulate and easily produced a clear cross section when broken, indicating reduced tensile strength for this polymer. The PPT (Figure 4A) film was also very thin due to its low efficiency of polymerization and appears as a mat of small globular particles. A very porous structure was obtained for PBrPT (Figure 4D), and the film thickness was about 7 times that for PCPT film. By decreasing the polymerization charge of the PCPT film to less than 100 mC/cm<sup>2</sup>, p- and n-doping charges became comparable indicating that the low

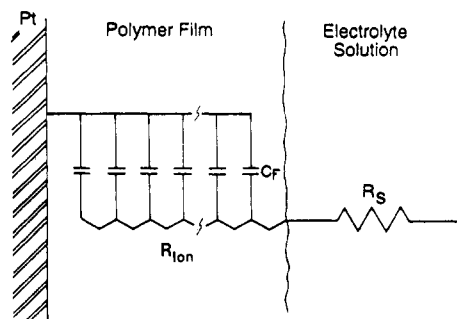


**Figure 6.** Equivalent circuit for polymer film-coated electrode according to the porous metal electrode model, where  $R_{ion}$  is the ionic resistance across the film thickness and  $R_s$  is the solution resistance.

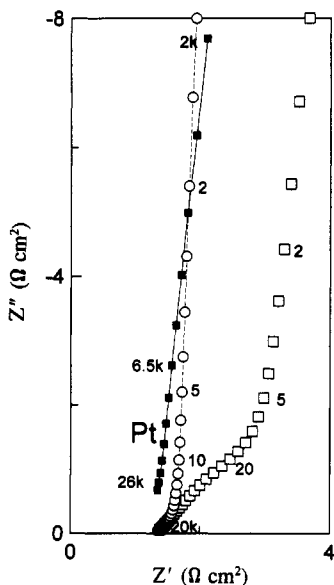


**Figure 7.** Complex plane impedance plots for the bare Pt electrode at open circuit potential (■) and the PFPT film coated Pt electrode at 0.7 V (○) and -1.9 V (□) in 0.2 M Et<sub>4</sub>NBF<sub>4</sub> acetonitrile solution.

n-doping charge of thicker PCPT films might be due to the slow ion transport rate (insertion of large cations) through the dense film. Similarly, we also found that the n-doping process was observed on only thin films of PT and P3MT. This prompted us to measure the ion-transport resistance for PCPT and PFPT films with impedance spectroscopy (vide infra).

In most cases a prepeak was observed for both n- and p-doping processes. Prepeaks for polythiophene have been previously explained using a charge trapping model<sup>18</sup> that was initially discovered by Murray and co-workers<sup>19,20</sup> on bilayer films of redox polymers. We also observed that the size of the prepeaks was dependent on the current density for growth, and the condition of the film, increasing as the polymer film deteriorated. Figure 5B shows the size of the prepeak and main peaks as a function of the polymerization current density for PFPT. This plot shows there is an optimal current density for the polymerization of this monomer. During the polymerization process, the initial polymer film formed on the electrode is exposed to

(18) Borjas, R.; Buttry, D. A. *Chem. Mater.* 1991, 3, 872.

(19) Abruna, H. D.; Denisevich, P.; Umana, M.; Meyer, T. J.; Murray, R. W. *J. Am. Chem. Soc.* 1981, 103, 1.

(20) Denisevich, P.; Willman, K. W.; Murray, R. W. *J. Am. Chem. Soc.* 1981, 103, 4727.

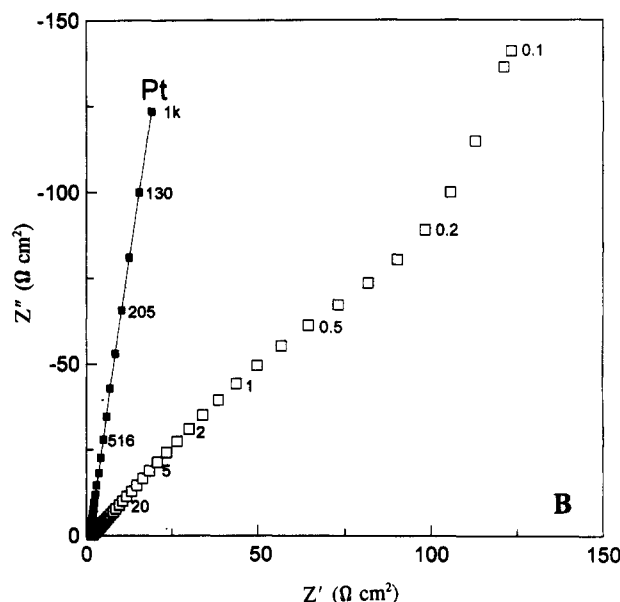
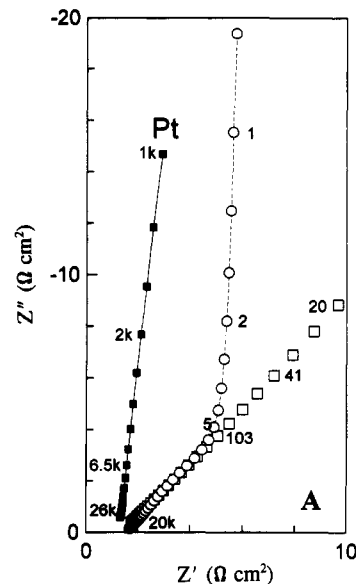


**Figure 8.** Complex plane impedance plots for the bare Pt electrode at open circuit potential (■) and the PCPT film coated Pt electrode at 0.7 V (○) and -1.9 V (□) in 0.2 M Et<sub>4</sub>NBF<sub>4</sub> acetonitrile solution.

**Table 2.** Ionic Resistances for PFPT and PCPT Films Measured with Impedance Spectroscopy

potential V vs Ag <sup>+</sup> /Ag	film ionic resistance (Ω cm <sup>2</sup> )	
	PFPT	PCPT
0.70	1.11	12.0
-1.90	4.8	>288

the high electrode potential required to oxidize the monomer. When polymerized at low current densities, the film is subjected to this high potential for a prolonged time which results in large prepeaks and diminished polymerization efficiency due to the loss of oligomers into solution. At high current densities (>14.2 mA/cm<sup>2</sup>), concentration limited polymerization arises, and a very high electrode potential is required to sustain the large current flow. Large prepeaks again were observed. The issue of the origin of the prepeaks and their relation to polymer stability cannot be dismissed since type III supercapacitors will be required to sustain 10<sup>5</sup> cycles. We are continuing our studies on this subject.

**Impedance Spectroscopy (IS) of PFPT and PCPT.** Since the first use of IS in the study of polypyrrole film-coated electrodes by Bard and co-workers in 1982,<sup>21</sup> this technique has been widely used to study conducting polymers.<sup>21-39</sup> Compared to cyclic voltammetry and other techniques involving a large potential perturbation, IS has the advantage of displacing the system only slightly from its equilibrium state with 5–10-mV peak-to-peak sinusoidal signals.<sup>33,40</sup> Also, by varying the frequency of the perturbation signals over a wide range, electrochemical processes with different time constants, such as interfacial and bulk phenomena, can be separated and studied. The system's impedance response is analyzed according to an equivalent circuit which contains elements such as resistors, capacitors, and sometimes inductors. It has been established for an electrode coated with a conducting layer, the slow ion movement in the solution pores can be studied using a porous metal electrode (PME) model.<sup>21,41-46</sup> The mathematical form of the impedance response is as follows:<sup>42</sup>

$$Z = \sqrt{\frac{R_{\text{ion}}}{j\omega C}} \coth \sqrt{j\omega R_{\text{ion}} C}$$

where  $R_{\text{ion}}$  is the total ionic resistance in the pore, and  $C$  is the total distributed interfacial capacitance of the pore. The equivalent circuit for this impedance is the simple transmission line shown in Figure 6.

PFPT and PCPT polymer films exhibited low electronic resistance when they were either nearly fully oxidized ( $E$

$> 0.45$  V) or nearly fully reduced ( $E < -1.8$  V). The charging rates of these polymer films were limited by the slow ion transport rate, thus the PME model is applicable to interpret the impedance data. In the potential range between  $-1.7$  and  $0.3$  V, the polymer films showed very low electronic conductivity and no electrochemical activity. Figure 7 shows the complex plane impedance plots for the PFPT film coated Pt electrode and a bare Pt electrode immersed in  $0.2$  M  $\text{Et}_4\text{NBF}_4$  acetonitrile solution. For both the oxidized form ( $E = 0.7$  V) and the reduced form ( $E = -1.9$  V), the impedance spectra displayed near ideal shapes, i.e., the high-frequency data form a straight line with a  $45^\circ$  angle to the axis of real impedance, and the low-frequency data lie on a vertical line for an ideal capacitor. Thus, the redox reaction induced by the ac potential wave at high-frequency starts at the polymer/solution interface.<sup>22,47</sup> Consequently, both the polymer film coated Pt electrode and the bare Pt electrode give the uncompensated solution resistance. As the frequency is decreased, the redox reaction layer expands inward from the polymer/solution interface, and the corresponding impedance data form a  $45^\circ$  Warburg-type line. At very low frequencies, the redox reaction layer encompasses the whole polymer film which remains in equilibrium with the changing potential, and the data form a vertical line in the complex impedance plane. Similar impedance plots were obtained for the PCPT film (Figure 8). The projected length of the  $45^\circ$  Warburg-type line on the real impedance axis characterizes the slow ion migration process in the solution pores and equals  $R_{\text{ion}}/3$ . The film ionic resistances evaluated from the impedance plots are listed in Table 2.

For both PFPT and PCPT films, the n-doping process had a higher ionic resistance than the p-doping process. Since the oxidation of the polymer chains involves the insertion of the electrolyte anions, and the reduction of the polymer chains involves the insertion of the electrolyte cations,<sup>5,18</sup> the IS results demonstrate that the cation insertion was more difficult than the anion insertion for both PFPT and PCPT polymer films. Compared to the PFPT film, the PCPT film had a very high ionic resistance for both n- and p-doping processes, consistent with its denser morphology. Since the film thickness limited capacitance behavior was only reached at a frequency lower than  $0.1$  Hz (Figure 8B), which corresponds to a scan rate less than  $2$  mV/s, the small cyclic voltammetric peaks for the n-doping process of the PCPT at scan rates  $> 20$  mV/s are thus understood to be a consequence of slow cation movement in the film. We are currently examining this transport using the electrochemical quartz crystal microbalance.

**Acknowledgment.** This work was supported by the Department of Energy Advanced Industrial Materials (AIM) and Electric/Hybrid Propulsion Programs through Los Alamos National Laboratory and the Petroleum Research Fund, administered by the American Chemical Society. We thank Jan A. Cowles for preparing several of the monomers.

- (21) Bull, R. A.; Fan, F. R. F.; Bard, A. J. *J. Electrochem. Soc.*, **1982**, *129* (5), 1009.  
 (22) Ren, X.; Pickup, P. G. *J. Phys. Chem.* **1993**, *97*, 3941.  
 (23) Ren, X.; Pickup, P. G. *J. Chem. Soc., Faraday. Trans.* **1993**, *89*, 321.  
 (24) Ren, X.; Pickup, P. G. *J. Phys. Chem.* **1993**, *97*, 5356.  
 (25) Ren, X.; Pickup, P. G. *J. Electrochem. Soc.* **1992**, *139*, 2097.  
 (26) Pickup, P. G. *J. Chem. Soc., Faraday. Trans.* **1990**, *86*, 3631.  
 (27) Duffitt, G. L.; Pickup, P. G. *J. Phys. Chem.* **1991**, *95*, 9634.  
 (28) Panero, S.; Prosperi, P.; Zane, D.; Scrosati, B. *J. Appl. Electrochem.* **1992**, *22* (3), 189.  
 (29) Miller, D. L.; Bockris, J. O. *J. Electrochem. Soc.* **1992**, *139* (4), 967.  
 (30) West, K.; Zachachristiansen, B.; Jacobsen, T.; Skaarup, S. *Mater. Sci. Eng.: B Solid State Mater. Adv. Technol.* **1992**, *13* (3), 229.  
 (31) Tanguy, J.; Baudoin, J. L.; Chao, F.; Costa, M. *Electrochim. Acta* **1992**, *37* (8), 1417.  
 (32) Tanguy, J.; Hoclet, M. *Synth. Met.* **1991**, *43* (1-2), 2995.  
 (33) Penner, R. M.; Martin, C. R. *J. Phys. Chem.* **1989**, *93* (2), 984.  
 (34) Musiani, M. M. *Electrochim. Acta* **1990**, *35*, 1665.  
 (35) Naoi, K.; Lien, M. M.; Smyrl, W. H.; Owens, B. B. *Appl. Phys. Commun.* **1989**, *9* (3), 147.  
 (36) Tanguy, J.; Slama, M.; Hoclet, M.; Baudouin, J. L. *Synth. Met.* **1989**, *28* (1-2), C145.  
 (37) Amemiya, T.; Hashimoto, K.; Fujishima, A. *J. Phys. Chem.* **1993**, *97*, 4187.  
 (38) Amemiya, T.; Hashimoto, K.; Fujishima, A. *J. Phys. Chem.* **1993**, *97*, 4192.  
 (39) Tanguy, J.; Slama, M.; Hoclet, M.; Baudouin, J. L. *Synth. Met.* **1989**, *28*, C145.  
 (40) Penner, R. M.; Van Dyke, L. S.; Martin, C. R. *J. Phys. Chem.* **1988**, *92* (18), 5274.  
 (41) Burgmayer, P.; Murray, R. W. *J. Phys. Chem.* **1984**, *88* (12), 2515.  
 (42) Jakobs, R. C. M.; Janssen, L. J. J.; Barendrecht, E. *Recl. J. R. Netherlands. Chem. Soc.* **1984**, *103*, 275.  
 (43) Waller, A. M.; Compton, R. G. *J. Chem. Soc., Faraday. Trans. 1* **1989**, *85*, 977.  
 (44) Paulse, C. D.; Pickup, P. G. *J. Phys. Chem.* **1988**, *92* (24), 7002.  
 (45) Mao, H.; Ochmanska, J.; Paulse, C. D.; Pickup, P. G. *Faraday. Discuss. Chem. Soc.* **1989**, *88*, 165.  
 (46) Pickup, P. G.; Murray, R. W. *J. Electrochem. Soc.* **1984**, *131*, 833.

- (47) Lee, C.; Kwak, J.; Bard, A. J. *J. Electrochem. Soc.* **1989**, *136*, 3720.